



# Diffusion kurtosis imaging in the characterisation of rectal cancer: utilizing the most repeatable region-of-interest strategy for diffusion parameters on a 3T scanner

Yiqun Sun<sup>1,2,3</sup> · Qin Xiao<sup>1,2</sup> · Feixiang Hu<sup>1,2</sup> · Caixia Fu<sup>4</sup> · Huixun Jia<sup>2,5</sup> · Xu Yan<sup>6</sup> · Chao Xin<sup>1,2</sup> · Sanjun Cai<sup>2,7</sup> · Weijun Peng<sup>1,2</sup> · Xiaolin Wang<sup>3</sup> · Tong Tong<sup>1,2</sup> · Yajia Gu<sup>1,2</sup>

Received: 21 October 2017 / Revised: 9 April 2018 / Accepted: 17 April 2018 / Published online: 24 May 2018

© European Society of Radiology 2018

## Abstract

**Objectives** Our goal was to investigate the correlation between histopathology and diffusion parameters by utilising the most repeatable region-of-interest (ROI) strategy for diffusion parameters in rectal cancer on a 3T scanner.

**Methods** 113 patients underwent DKI-MR and 66 of these patients received surgery without neoadjuvant chemoradiotherapy. Two readers independently measured the parameters using three slice protocols including single slice, three slices and whole-tumour slice (WTS), combined with one of two ROIs, including outline and round ROI. ANOVA, Kruskal-Wallis, a paired sample t-test, interclass correlation coefficient (ICC), Bland-Altman, Student's t-tests, receiver operating characteristic curves and z statistic were used for statistical analysis.

**Results** There were no significant differences among the three slice protocols in ADC values ( $p = 0.822, 0.987$ ), K values ( $p = 0.842, 0.859$ ) and D values ( $p = 0.917, 0.988$ ) using round and outline ROI, respectively. The ADC and D values derived from outline ROIs were higher than those from round ROIs (all  $p < 0.001$  for ADC, all  $p < 0.001$  for D), while K values derived from outline ROIs were lower than those from round ROIs ( $p < 0.001, p = 0.001, p < 0.001$ ) using three slice protocols, respectively. The WTS-outline ROI resulted in the best intra- and inter-observer ICC. Utilising the WTS-outline ROI method, the AUC for assessment of well-differentiated tumours was 0.871 by K and 0.809 by ADC; and the AUC for T2 was 0.768 by K.

**Conclusions** The most repeatable strategy was the WTS-outline ROI method. In addition to DWI, DKI also have diagnostic value for rectal cancer histopathological characteristics utilising the WTS-outline ROI on a 3T scanner.

## Key Points

- DKI using a 3T scanner is feasible for assessing rectal cancer.
- ROI and slice protocol show considerable influence on DKI parameters.
- DKI parameters exhibit excellent repeatability using whole-tumour slice-outline ROI on 3T scanner.
- DKI has considerable diagnostic value for the estimation of rectal cancer characteristics.

**Keywords** Rectal neoplasms · Diffusion magnetic resonance imaging · Reproducibility of results · Biomarkers · Feasibility studies

---

Yiqun Sun and Qin Xiao contributed equally to this work and are co-first authors.

---

✉ Tong Tong  
t983352@126.com

✉ Yajia Gu  
cjr.guyajia@vip.163.com

<sup>1</sup> Department of Radiology, Fudan University Shanghai Cancer Center, 270 Dong An Road, Shanghai 200032, China

<sup>2</sup> Department of Oncology, Shanghai Medical College, Fudan University, Shanghai, China

<sup>3</sup> Shanghai Institute of Medical Imaging, Fudan University, Shanghai, China

<sup>4</sup> Siemens Shenzhen Magnetic Resonance Ltd., Shenzhen, China

<sup>5</sup> Department of Clinical Statistics Center, Fudan University Shanghai Cancer Center, Shanghai, China

<sup>6</sup> MR Collaboration NE Asia, Siemens Healthineer, Shanghai, China

<sup>7</sup> Department of Colorectal Surgery, Fudan University Shanghai Cancer Center, Shanghai, China

## Abbreviations

ADC	Apparent diffusion coefficient
AJCC	American Joint Committee on Cancer
AUC	Area under curve
BA-LA	Bland-Altman limits of agreements
CRM	Circumferential resection margin
D	Corrected diffusion coefficient
DKI	Diffusion kurtosis imaging
DWI	Diffusion weighted imaging
EPI	Single-shot echo-planar imaging
ICC	Interclass correlation coefficient
K	Diffusion kurtosis coefficient
LVI	Lymphovascular invasion
MRI	Magnetic resonance imaging
NCRT	Neoadjuvant chemoradiotherapy
ROC	Receiver operating characteristic
ROI	Region of interest
SD	Standard deviation
SNR	Signal-to-noise ratio
SS	Single slice
T2WI	T2-weighted images
TS	Three slices
TSE	Turbo spin echo
WHO	World Health Organization
WTS	Whole tumour slice

## Introduction

Several studies have demonstrated that DKI not only performed better than conventional ADC values in the detection and grading of various lesions, but also identified early microstructural changes in tissues and could assess treatment responses [1–6]. Zhu et al. [6] demonstrated that the kurtosis parameter from the DKI model yields a higher correlation with histological grades compared to the diffusivity and ADC of rectal adenocarcinomas using 1.5T scanner. However, it has been established that a single-shot EPI DWI sequence is very sensitive to susceptibility artifacts, which are more severe on 3T versus 1.5T systems, due to the imperfect B<sub>0</sub> field homogeneity. The susceptibility artifact might reduce the performance of DKI in characterising rectal lesions. Thus, it is important and necessary to verify that the DKI model could have equal performances on the 1.5T and 3T systems.

The repeatability of DKI measurements in rectal cancer needs to be evaluated on a 3T scanner, because standardising the ROI is the first step in clinical application. However, some studies have shown that the size and the positioning of the region of interest (ROI) influenced the statistical results of DWI parameters and their inter-observer variability [7–10]. Lambregts et al. [7] reported that the most reproducible results were obtained when measuring the ADC of the whole-tumour volume for rectal cancer based on their study conducted at

1.5T. Compared with conventional DWI, the DKI sequence utilises higher diffusion gradients to implement higher b values (normally a maximum b value of > 2,000 mm<sup>2</sup>/s is required), which might result in more image distortions due to the eddy current caused by the high magnetic gradient pulse. Therefore, whether the whole-tumour volume strategy could help generate more reproducible results for DKI, especially at 3T, needs to be confirmed. Moreover, DKI-derived parameter Kurtosis and conventional ADC refer to different phenomena of the tumour microstructure [11–13]. It is necessary to explore the most repeatable ROI strategy for diffusion kurtosis imaging parameters in rectal cancer.

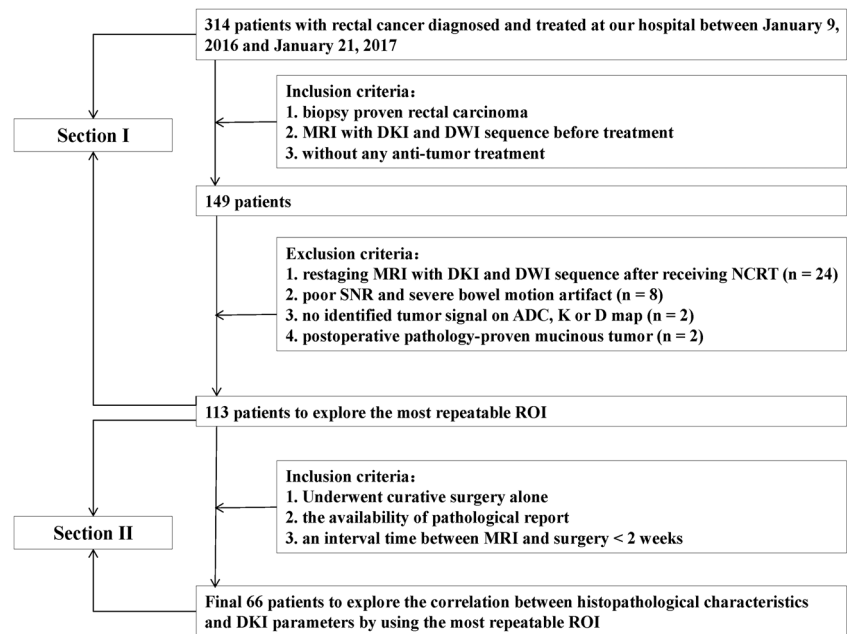
Thus, the objective of this study was to explore the influence of different ROI strategies on the measurement of diffusion parameters using a 3T scanner. We examined DKI and conventional DWI to access the correlation between these diffusion parameters from the most repeatable ROI strategy for identifying rectal cancer characteristics.

## Materials and methods

### Patients

Institutional review board approval was obtained for this retrospective study. 314 patients with rectal cancer who were diagnosed and treated at our hospital between 9 January 2016 and 21 January 2017 were selected for review in our study. Inclusion criteria were: (1) biopsy-proven rectal adenocarcinoma, (2) evaluation MRI with DKI and DWI sequence before treatment, and (3) the absence of any anti-tumour treatment. 149 patients who met the inclusion criteria were selected. Exclusion criteria were: (1) restaging MRI with DKI and DWI sequence after receiving neoadjuvant chemoradiotherapy (NCRT) (n=24), (2) poor signal-to-noise ratio (SNR) and severe bowel motion artifacts (n=8), (3) no identified tumour signal on ADC, K or D map (n=2), and (4) a postoperative pathology-proven mucinous tumour (n = 2). In total, 113 patients (64 male, 49 female) with a median age of 59 years (range: 27–86 years) were enrolled to explore the most repeatable tumour strategy on DKI in the first section. A subgroup of the patients was selected for the second section using the following selection criteria: (1) underwent curative surgery alone, (2) the pathological reports were available, and (3) the time interval between MRI and surgery was less than 2 weeks. Finally, there were 66 patients (41 male, 25 female), with a median age of 61 years (range: 30–83 years) in the second section. Clinical and imaging data were retrieved from a patient database. The workflow is displayed in Fig. 1.

Fig. 1 The workflow



### MRI technique

All MRIs were performed on a 3T MR scanner (MAGNETOM Skyra, Siemens Healthineers) with a 16-channel phase-array body coil. The MRI protocol mainly included a sagittal T2-weighted TSE (turbo spin echo), an oblique axial thin-section T2-weighted TSE, and an oblique axial multi-b EPI (single-shot echo-planar imaging) DWI sequence. The multi-b EPI DWI sequence was performed using the following parameters: orientation = oblique axial; b values = 0, 700, 1,400 and 2,100 s/mm<sup>2</sup>; repetition time (TR)/echo time (TE) = 4,800/79 ms; parallel imaging factor = 2; fat suppression = spectral adiabatic inversion recovery; field of view (FOV) = 240×180 mm<sup>2</sup>; matrix = 120×120; section thickness = 5.5 mm; number of sections = 20; no. of average = 1, 2, 4 and 6 (for 0, 700, 1,400 and 2,100 s/mm<sup>2</sup> respectively); Bandwidth = 1,894 Hz/pixel. Patients did not receive any bowel preparation before the MRI examinations.

The parameter maps of DKI (corrected diffusion coefficient, D; diffusion kurtosis coefficient, K) and conventional DWI (apparent diffusion coefficient, ADC) were calculated from the multi-b DWI data with all measured b values by using prototype post-processing software Body Diffusion Toolbox (Siemens Healthineers). The multi-b DW images were fitted voxel-by-voxel using the DK signal decay equation:

$$S(b) = S_0 \times \exp(-bD + b^2 D^2 K / 6). \tag{1}$$

In this equation, S(b) is the signal intensity at a certain b-value, S<sub>0</sub> is the baseline signal without diffusion weighting, D is the corrected diffusion coefficient (unit: 10<sup>-3</sup>mm<sup>2</sup>/s), and K is the excess diffusion kurtosis coefficient. K describes the

degree to which molecular motion deviates from the perfect Gaussian distribution. When K is equal to 0, equation (1) degrades to a conventional monoexponential equation:

$$S(b) = S_0 \times \exp(-b \times ADC). \tag{2}$$

The difference between D and ADC is that D is a corrected form of ADC (unit: 10<sup>-3</sup>mm<sup>2</sup>/s) for use in non-Gaussian circumstances.

### Image analysis

Two radiologists (TT and SYQ, with 10 and 4 years of experience in rectal cancer imaging, respectively), blind to the clinical patient data and pathological report, drew ROIs on axial ADC maps independently. The tumour was defined as a focal mass showing low signal intensity on an ADC map compared with the signal from the adjacent tissue and exhibited high signal intensity on DWI and intermediate signal intensity on the anatomical T2-weighted images (T2WI). Each radiologist performed the measurements twice at 1-month intervals.

Two different ROIs were positioned on the slice (Fig. 2): (1) round ROI: a round ROI was manually placed within solid tumour parts in the largest possible area and (2) outline ROI: a freehand ROI was drawn along the border of the lower signal of the tumour to cover the entire tumour area on each slice. Both round and outline ROIs excluded visible necrosis, the intestinal lumen and artifacts. The number of slices with ROI placement was determined by three protocols: (1) single slice (SS): one slice with the largest area of tumour, (2) three slices (TS): containing (a) and its adjacent upper and lower slice, and (3) whole-tumour slice (WTS): all slices of the tumour. ROIs

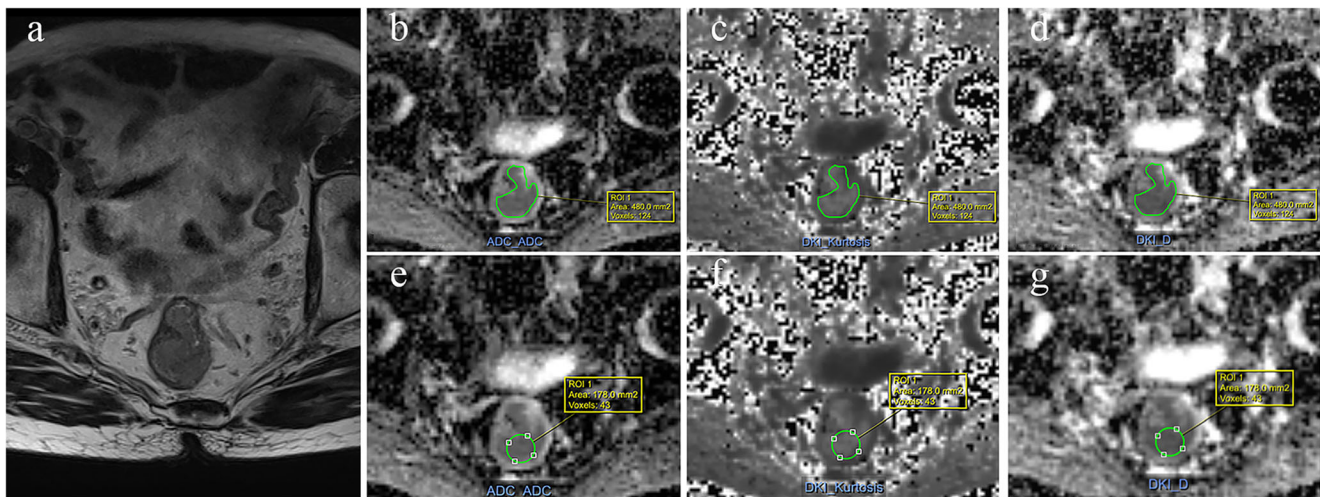


**Fig. 2** A 38-year-old woman with rectal cancer, as shown on the axial T2WI (a), outline ROI (green hand-drawn lines) on the ADC map (b), round ROI (green circle) on ADC map (e), outline ROI on K map (c),

round ROI on K map (f), outline ROI on D map (d), round ROI on D map (g)

were copied to K and D maps automatically by the software. Mean ADC, D and K values were obtained for each reader in each case.

### Histopathology evaluation

A gastrointestinal pathologist with 8 years of experience, who was unaware of other clinical or molecular data, reviewed haematoxylin- and eosin-stained tissue sections from all rectal cancer cases. The histopathology factors included histological grade, T category, N category, circumferential resection margin (CRM), perineural invasion and lymphovascular invasion (LVI). The tumour category was determined according to the TNM classification system recommended by the International Union against Cancer and the American Joint Committee on Cancer (AJCC), 7th ed., 2010 [14].

### Statistical analysis

All continuous variables as diffusion parameters and ROI are average values among readers. The Kolmogorov–Smirnov test was used to ascertain the distribution of continuous numeric data. Moreover, the distribution of measurement in all methods and based on histopathological factors was normal, except for the measurable data of T1, N2 and CRM (positive) not normally distributed. The data were provided as the mean  $\pm$  standard deviation (SD) with normal distribution. The median value and interquartile range (IQR) were described with no normal distribution. The ANOVA test was used to compare the diffusion parameters of the three different slice protocols. A paired sample t-test was used to compare round and outline ROI diffusion parameters.

The first and second measurements of radiologist SYQ were used to analyse the intra-observer variability. The first

measurements of radiologist SYQ and radiologist TT were used to analyse the inter-observer variability. The intra- and inter-observer variability for the ADC, K and D values were evaluated using the intraclass correlation coefficient (0.00–0.20 poor, 0.21–0.40 fair, 0.41–0.60 moderate, 0.61–0.80 good and 0.81–1.00 excellent correlation). In addition, Bland-Altman plots with limits of intra- and inter-reader agreement (mean difference  $\pm$  1.96  $\times$  SD) were used for graphical representation of the data. The most repeatable strategy was selected based on intra-observer and inter-observer variability. The averaged ADC, K and D values of two radiologists were used for the next part of this study.

Student's t-tests (independent-samples t-test) were used to assess the differences of diffusion parameters based on histological grade, PNI and LVI. Kruskal-Wallis tests were used to assess differences in diffusion parameters based on T, N and CRM categories. The sensitivity, specificity and area under the curve (AUC) of the receiver operating characteristic (ROC) for evaluation of histopathological factors were also calculated. The pairwise comparison of ROC curves between the DKI and conventional DWI models was performed using z statistic. Cut-off values were established by calculating the maximal Youden index: Youden index = sensitivity - (1-specificity).

Statistical analysis was performed using SPSS (version 21.0; SPSS) and MedCalc (version 12.7.2; MedCalc Software). *P* values < 0.05 were considered statistically significance.

## Results

### Patient characteristics

A total of 113 patients were analysed in the present study. The study population was mainly male (56.6 %) with a median age

of 59 years (range 27–86 years). In all, there were 47 (41.6%) patients who received NCRT followed by surgery and 66 (58.4%) patients who received curative surgery alone. The patient characteristics are summarised in Table 1.

**The mean and SD of the thickness and the size of the ROIs**

The mean thickness of the round and outline ROI was 40.5 ± 12.4 mm and 45.0 ± 12.6 mm using WTS, respectively. The mean size of the round ROI was 302.0 ± 106.1 mm<sup>2</sup>, 223.2 ± 79.9 mm<sup>2</sup> and 177.5 ± 87.9 mm<sup>2</sup> in the single slice, three slices and WTS methods, respectively. The mean size of the outline ROI was 591.7 ± 192.1 mm<sup>2</sup>, 493.4 ± 179.5 mm<sup>2</sup> and 371.6 ± 177.5 mm<sup>2</sup> for the single slice, three slices and WTS methods, respectively.

**Effect of slice protocols on ADC, K and D values**

The statistics were based on diffusion parameters, which were the average of two readers’ measurements. The diffusion parameters using different slice protocols are shown in Table 2. In analysing the whole study population, there were no significant differences in the ADCs derived from different slice protocols (*p* = 0.822, 0.987 using round and outline ROI, respectively), and the same results were observed for K (*p* = 0.842, 0.859 using round and outline ROI, respectively) and D (*p* = 0.917, 0.988 using round and outline ROI, respectively) values. Therefore, the slice protocols were not significantly influenced by ADC, K and D values.

**Effect of ROI on ADC, K and D values**

Similarly, the statistical diffusion parameters were the average of two readers’ measurements. The diffusion parameters using different ROIs are shown in Table 3. Tumour ADC values from outline ROIs were significantly higher than those from round ROIs (*p* < 0.001, using single slice, three slices and WTS, respectively). Tumour D values from outline ROIs were also significantly higher than those from round ROIs (*p* < 0.001 using single slice, three slices and WTS, respectively). K values derived from the round ROIs were significantly higher than those from the outline ROIs (*p* < 0.001, =0.001, < 0.001 using single slice, three slices and WTS, respectively). Therefore, the ROI had considerable influence on the ADC, K and D values.

**The intra- and inter-observer variability of ADC, K and D values for the different strategies**

The intra- and inter-observer variability of ADC, K and D values for the different strategies are given in Table 4. On the whole, the intra- and inter-observer ICCs were excellent for the ADC (0.965, 0.825, respectively), K (0.909, 0.945, respectively) and D (0.902, 0.874, respectively) using WTS-outline ROI. For the remaining ROI protocols, the intra-observer and inter-observer variabilities were not better than for the WTS-outline ROI. Overall, the WTS-outline ROI strategy had the lowest limits of agreement (+0.05/-0.05, +0.11/-0.13 for ADC intra- and inter-observer, +0.08/-0.10, +0.12/-0.13 for K intra- and inter-observer and +0.22/-0.16, +0.24/-

**Table 1** Demographics of the patients

		Number	%			Number	%	
All patients enrolled		113	100%	Histopathological finding of patients receiving curative surgery alone		66	100%	
Age	Median (y)	59		Histological grade		Poorly-moderately differentiated	59	89.4%
	Range (y)	27–86				Well differentiated	7	10.6%
Gender	Male	64	56.6%	Pathology T category		T1	5	7.6%
	Female	49	43.4%			T2	24	36.3%
Treatment	NCRT followed by surgery	47	41.6%			T3	37	56.1%
	Curative surgery alone	66	58.4%	Pathology N category		N0	39	59.1%
						N1	20	30.3%
						N2	7	10.6%
				CRM		Negative	64	97%
						Positive	2	3%
				Perineural invasion		Negative	49	74.2%
						Positive	17	25.8%
				LVI		Negative	59	89.4%
						Positive	7	10.6%

NCRT neoadjuvant chemoradiotherapy, CRM circumferential resection margin, LVI lymphovascular invasion

**Table 2** Comparison of three different slice-based protocols for ADC, K and D values

Slice protocol	ADC $\times (10^{-3}\text{mm}^2/\text{s})$		K		D $\times (10^{-3}\text{mm}^2/\text{s})$	
	Round ROI	Outline ROI	Round ROI	Outline ROI	Round ROI	Outline ROI
Single slice (1)	0.661 $\pm$ 0.099	0.685 $\pm$ 0.094	1.009 $\pm$ 0.117	0.979 $\pm$ 0.109	1.154 $\pm$ 0.221	1.197 $\pm$ 0.214
Three slices (2)	0.668 $\pm$ 0.094	0.685 $\pm$ 0.095	1.002 $\pm$ 0.113	0.973 $\pm$ 0.109	1.162 $\pm$ 0.211	1.196 $\pm$ 0.218
WTS (3)	0.668 $\pm$ 0.095	0.687 $\pm$ 0.095	1.000 $\pm$ 0.112	0.971 $\pm$ 0.108	1.167 $\pm$ 0.215	1.204 $\pm$ 0.220
<i>p</i>	0.822	0.987	0.842	0.859	0.917	0.988

ROI region of interest, WTS whole tumour slice, ADC apparent diffusion coefficient, K diffusion kurtosis coefficient, D corrected diffusion coefficient

0.24 for D intra- and inter-observer respectively) among the six strategies. The above results showed the most repeatable strategy is the WTS-outline ROI. Figure 3 shows the Bland-Altman plots for the WTS-outline ROI measurements performed.

### The correlation between histopathological characteristics of rectal cancer and diffusion parameters derived from the WTS-outline ROI

The diffusion parameters were used to explore the correlation with the histopathological characteristics of rectal cancer, and the average of the two readers' measurements utilising the most repeatable strategy, namely the WTS-outline ROI method. The correlation between histopathological characteristics and diffusion parameters is shown in Table 5. The ADC of poorly to moderately differentiated tumours ( $0.664 \pm 0.066$ )  $\times 10^{-3}\text{mm}^2/\text{s}$  was lower than in well differentiated tumours ( $0.721 \pm 0.064$ )  $\times 10^{-3}\text{mm}^2/\text{s}$  ( $p = 0.034$ ), but trends for K show the opposite effect ( $0.993 \pm 0.105$  vs.  $0.905 \pm 0.059$ ) ( $p = 0.037$ ). K is different in the T1-3 category. There were significant differences between T1 and T2 ( $0.814$  ( $0.773$ – $1.052$ ) vs.  $0.998 \pm 0.086$ ,  $p = 0.007$ ) and T1 and T3 ( $0.814$  ( $0.773$ – $1.052$ ) vs.  $0.991 \pm 0.106$ ,  $p = 0.008$ ), while the difference between T2 and T3 ( $0.998 \pm 0.086$

vs.  $0.991 \pm 0.106$ ) was not significant ( $p = 0.782$ ). For T category, there was no significant difference in the ADC and D values. The ADC, K and D values were different in the subgroups based on N category, CRM, perineural invasion and LVI, but these differences were not statistically significant ( $p > 0.05$ ).

### Performance of ADC, K and D values to distinguish characteristics of rectal cancer

Similarly, the diffusion parameters are the average of the two readers' measurements utilising the WTS-outline ROI. The ROC curves were used to assess the diagnostic performance of the parameters of DKI and conventional DWI for the assessment of tumour characteristics. The AUC was 0.809 (95% CI: 0.693–0.895,  $p < 0.001$ ) and 0.871 (95% CI: 0.766–0.941,  $p < 0.001$ ) for the assessment of well differentiated tumours using the ADC and K values, respectively, and there was no significant difference between them ( $p = 0.276$ ) (Fig. 4). The optimal cut-off value was 0.959 for K (100% sensitivity and 66.67% specificity) and  $0.697 \times 10^{-3}\text{mm}^2/\text{s}$  for ADC (77.78% sensitivity and 77.19% specificity). The AUC was 0.768 (95% CI: 0.592–0.914,  $p = 0.04$ ) for distinguishing T2 from T1 by K values (Fig. 5). The optimal cut-off value was 0.908, which showed relatively high sensitivity (81.1%) and specificity (80%).

**Table 3** Comparison of round and outline ROI for ADC, K and D values

Slice protocol		ADC $\times (10^{-3}\text{mm}^2/\text{s})$	K	D $\times (10^{-3}\text{mm}^2/\text{s})$
Single slice	Round ROI	0.661 $\pm$ 0.099	1.009 $\pm$ 0.117	1.154 $\pm$ 0.221
	Outline ROI	0.685 $\pm$ 0.094	0.979 $\pm$ 0.109	1.197 $\pm$ 0.214
	<i>p</i>	<0.001	<0.001	<0.001
Three slices	Round ROI	0.668 $\pm$ 0.094	1.002 $\pm$ 0.113	1.162 $\pm$ 0.211
	Outline ROI	0.685 $\pm$ 0.095	0.973 $\pm$ 0.109	1.196 $\pm$ 0.218
	<i>p</i>	<0.001	<0.001	0.001
WTS	Round ROI	0.668 $\pm$ 0.095	1.000 $\pm$ 0.112	1.167 $\pm$ 0.215
	Outline ROI	0.687 $\pm$ 0.095	0.971 $\pm$ 0.108	1.204 $\pm$ 0.220
	<i>p</i>	<0.001	<0.001	<0.001

ROI region of interest, WTS whole tumour slice, ADC apparent diffusion coefficient, K diffusion kurtosis coefficient, D corrected diffusion coefficient

**Table 4** The intra- and inter-observer variability of ADC, K and D values for the different strategies

Slice protocol	ROI	ADC Intra-observer		K Intra-observer		D Intra-observer	
		ICC <sup>#</sup>	Mean difference (+1.96SD/-1.96SD)	ICC	Mean difference (+1.96SD/-1.96SD)	ICC	Mean difference (+1.96SD/-1.96SD)
Single-slice	Round	0.753	-0.01 (+0.16/-0.14)	0.669	0.01 (+0.28/-0.26)	0.742	-0.01 (+0.35/-0.37)
	Outline	0.885	0.01 (+0.10/-0.08)	0.777	0.01 (+0.21/-0.19)	0.854	0.04 (+0.28/-0.20)
Three slices	Round	0.877	-0.00 (+0.10/-0.10)	0.785	0.01 (+0.18/-0.16)	0.772	0.01 (+0.32/-0.30)
	Outline	0.939	0.00 (+0.07/-0.07)	0.888	-0.01 (+0.09/-0.11)	0.790	0.04 (+0.25/-0.17)
WTS	Round	0.946	0.00 (+0.06/-0.06)	0.850	0.01 (+0.15/-0.13)	0.866	0.03 (+0.24/-0.18)
	Outline	0.965	0.00 (+0.05/-0.05)	0.909	-0.01 (+0.08/-0.10)	0.902	0.03 (+0.22/-0.16)
		ADC Inter-observer		K Inter-observer		D Inter-observer	
		ICC	Mean difference (+1.96SD/-1.96SD)	ICC	Mean difference (+1.96SD/-1.96SD)	ICC	Mean difference (+1.96SD/-1.96SD)
Single-slice	Round	0.658	-0.01 (+0.18/-0.20)	0.548	0.01 (+0.26/-0.24)	0.620	0.02 (+0.45/-0.41)
	Outline	0.785	0.01 (+0.14/-0.12)	0.751	-0.03 (+0.16/-0.22)	0.709	0.05 (+0.39/-0.29)
Three slices	Round	0.761	-0.01 (+0.12/-0.14)	0.701	-0.01 (+0.13/-0.15)	0.670	0.01 (+0.39/-0.37)
	Outline	0.807	0.01 (+0.13/-0.11)	0.716	-0.01 (+0.13/-0.15)	0.747	0.05 (+0.38/-0.28)
WTS	Round	0.813	-0.03 (+0.09/-0.15)	0.768	0.01 (+0.15/-0.13)	0.727	0.01 (+0.36/-0.34)
	Outline	0.825	-0.01 (+0.11/-0.13)	0.945	-0.01 (+0.12/-0.13)	0.856	0.00 (+0.24/-0.24)

ICC: interclass correlation coefficient

SD: standard deviation

ROI: region of interest

WTS: whole tumour slice

ADC: apparent diffusion coefficient

K: diffusion kurtosis coefficient

D: corrected diffusion coefficient

<sup>#</sup>: 0.00–0.20 poor; 0.21–0.40 fair; 0.41–0.60 moderate; 0.61–0.80 good; 0.81–1.00 excellent correlation

## Discussion

In our study, different slice protocols do not significantly influence ADC, K and D measurements on the 3T system. Lambregts’s [7] study also demonstrated that there are no significant differences in tumour ADC values between whole-volume and single-slice methods, which is in agreement with our results. In cases where tumours are small, the number and selection of slices may not vary for different slice protocols. Furthermore, it is fairly simple to correctly define the largest tumour axial section on the ADC map to reduce selection bias, which also helps to explain our results.

However, different ROI methods have considerable influence on diffusion parameters. Tumour ADC and D values from outline ROIs are significantly higher than those from round ROIs. In addition, K values derived from the round ROI method are significantly higher than those from the outline ROI method. Chie et al. [15] also confirmed that the ADCs from outline ROIs are relatively higher than those from round ROIs. The outline ROI covers the whole tumour signal and therefore may contain relatively more micro-liquefactive necrosis, which cannot be distinguished by the naked eye, but can increase water diffusivity, contributing to a higher ADC and D value than round ROIs. For round ROIs, which were placed within the

solid tumour, there may exist a higher cell density and more complicated cell activity than for the outline ROI, which may in turn lead to higher K values.

Our study showed that the WTS-outline ROI measurement generated the highest intra- and inter-observer agreement of ADC, K and D on the 3T system. This result may be for the following reasons. First, rectal cancers normally have irregular shapes and the positioning of the round ROI within the solid tumour might vary among readers, while this variation can be minimised using an outline ROI method. Thus, there may be a difference in the absolute values among readers measured by round ROI, but not by outline ROI. Second, selection bias is further minimised using the whole tumour slice protocol. Third, analysing a larger number of pixels may result in more reproducible results for the measured parameters. We would therefore conclude that the most repeatable ROI strategy is not dependent upon diffusion-fitting model or magnetic field strength. Thus, we recommend the WTS-outline ROI strategy to measure the parameters of DKI, and we used this method for further analysis in our study.

By using WTS-outline ROI, K values in well-differentiated tumours were significantly lower than those in poorly to moderately differentiated tumours, which was consistent with the conclusion of Zhu’s study performed on a 1.5T system. While ADC values in poorly to moderately differentiated tumour

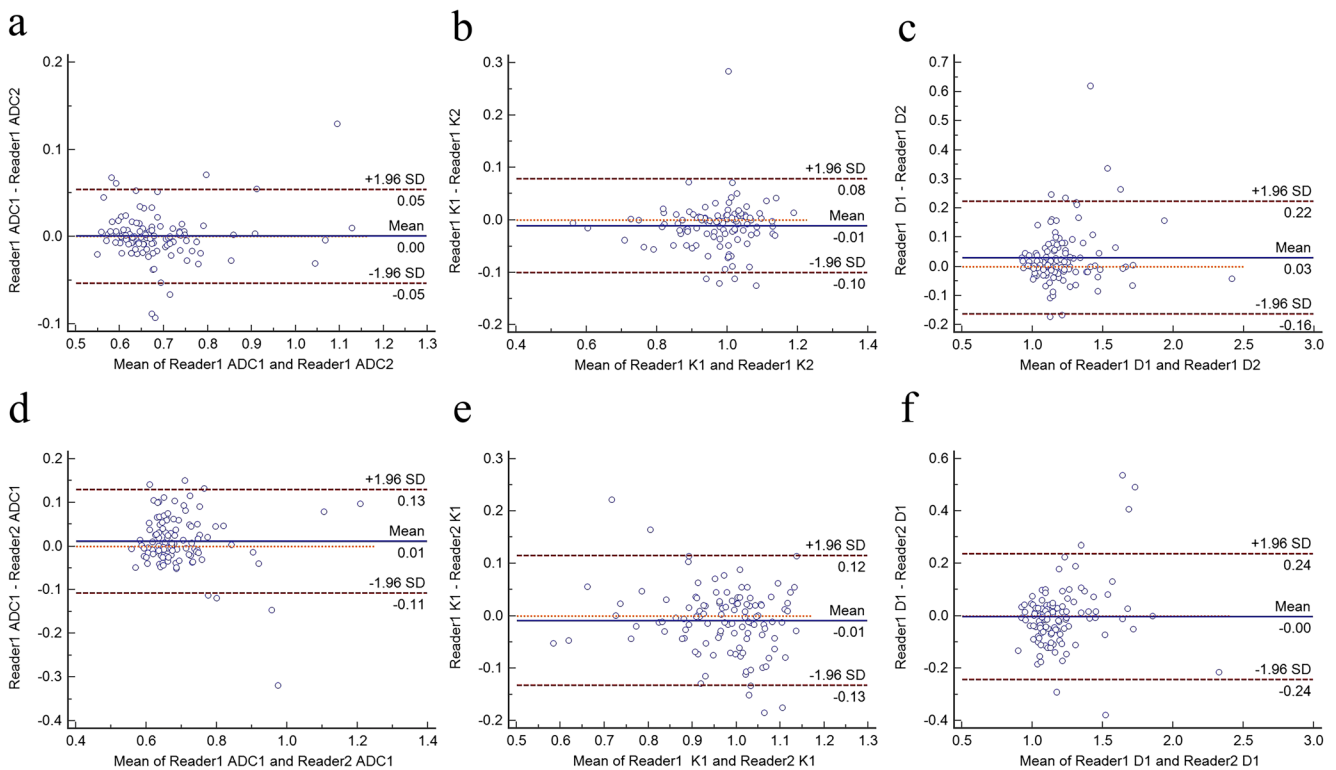


**Fig. 3** Bland-Altman plots show intra- and inter-observer agreement for ADC (a, d), K (b, e) and D (c, f) values measured by using WTS-outline ROI

were significantly lower than those in well-differentiated tumours, Akashi's [16], Curvo-Semedo's [17] and our previous study [18] also confirmed this finding. Compared to well differentiated tumours, poorly to moderately differentiated tumours are characterised by increased mitotic activity and varied nuclear pleomorphisms, resulting in few diffusion barriers and increased structural complexity. Thus, employing the differences in K and ADC observed in our study to reflect the differences in microstructural complexity and water diffusion between poorly to moderately and well differentiated tumours is possible. Of particular note, K values in T1 were significantly lower than in T2 and T3 tumours in our study. The AUC can distinguish T2 from T1 by K values, and K values also show relatively high sensitivity and specificity. How to identify T1 and T2 on MR before treatment remains a challenge. Our results show such K values will be useful in distinguishing T2 from T1 tumours when considering treatment strategies. The following reasons may explain the better performance of the DKI model compared with that of the DWI model. First, the conventional DWI model is based on the assumption that water diffusion within a voxel follows Gaussian behaviour, whereas the DKI model is based on another assumption that water molecules within biological tissues exhibit a non-Gaussian phenomenon, which provides a more accurate model of diffusion and captures the non-Gaussian diffusion behaviour as a reflective marker for tissue heterogeneity [19]. The vigorous cell mitosis and strong

proliferative ability in more aggressive cancers can result in more a complex microstructure and increased cell density in each voxel, which in turn affects water diffusion (vs. less aggressive tumours).

The results of other analyses, including ADC, K and D values between lymph node, perineural invasion and LVI-based subgroups did not show statistical significance and might be limited by sample size and imbalanced population distributions. Larger numbers of patients are needed to further explore the performance of ADC, K and D values in predicting histopathological characteristics.

Our study has some limitations. First, restaging MRI after NCRT was excluded in our study. The reason for exclusion was the number of the patients who underwent diffusion imaging after NCRT was very small and the regressive lesions were scarcely visible in diffusion images. Second, we did not use spasmolytic and endorectal gel to reduce susceptibility artifacts for diffusion imaging. The usage of spasmolytic and endorectal gel could increase the drawing accuracy of the outline ROI along the border of the tumour and increase the reliability of our conclusions. Third, the patient distribution in our study was uneven with only two patients exhibiting poor differentiation. Finally, we did not use an area-weighted averaging method to calculate the mean values of the measured parameters in TS and WTS protocols, which might influence the accuracy of our results. Thus, further study with a more accurate



**Table 5** Histopathological characteristic correlation with diffusion parameters derived from WTS-outline ROI in rectal cancers

Patients characteristic		Number	ADC ( $\times 10^{-3} \text{mm}^2/\text{s}$ )	<i>p</i>	K	<i>p</i>	D ( $\times 10^{-3} \text{mm}^2/\text{s}$ )	<i>p</i>
Histological grade	Poor-Mid	59	0.663 ± 0.066	0.034	0.993 ± 0.105	0.037	1.258 ± 0.232	0.267
	Well	17	0.720 ± 0.064		0.905 ± 0.059		1.165 ± 0.203	
Pathology T category	T1	5	0.729 (0.625-0.730)	0.097	0.814 (0.773-1.052)	0.007 <sup>###</sup>	1.157 (1.028-1.185)	0.663
	T2	24	0.662 ± 0.065	0.124	0.998 ± 0.086	0.782 <sup>####</sup>	1.150 ± 0.119	0.875
	T3	37	0.667 ± 0.070	0.743	0.991 ± 0.106	0.008 <sup>#####</sup>	1.183 ± 0.226	0.595
Pathology N category	N0	39	0.667 ± 0.071	0.946	0.986 ± 0.105	0.910	1.166 ± 0.177	0.486
	N1	20	0.666 ± 0.046	0.417	0.983 ± 0.101	0.731	1.224 ± 0.294	0.639
	N2	7	0.683 (0.630-0.768)	0.423	0.968 (0.900-1.013)	0.802	1.112 (1.057-1.500)	0.383
CRM	Negative	64	0.678 ± 0.059	0.722	0.978 ± 0.093	0.941	1.204 ± 0.184	0.562
	Positive	2	0.642(range:0.620-0.664) *		1.043(range:1.035-1.051) *		1.105(range:1.069-1.141) *	
PNI	Negative	49	0.666 ± 0.065	0.563	0.985 ± 0.105	0.807	1.207 ± 0.220	0.469
	Positive	17	0.677 ± 0.076		0.978 ± 0.106		1.164 ± 0.203	
LVI	Negative	59	0.667 ± 0.067	0.483	0.985 ± 0.104	0.705	1.182 ± 0.190	0.936
	Positive	7	0.688 ± 0.072		0.968 ± 0.119		1.175 ± 0.210	

ADC apparent diffusion coefficient, K diffusion kurtosis coefficient, D corrected diffusion coefficient, CRM circumferential resection margin, PNI perineural invasion, LVI lymphovascular invasion, ADC K and D values of T1, N2 and CRM (positive) were not normally distributed, the data were described with median value and interquartile range (IQR) instead of mean ± (standard deviation, SD)

\* We could not describe the IQR, but described the range of date because there were only two patients in this group.

<sup>###</sup> Indicates a significant difference when T1 K values are compared with T2

<sup>####</sup> Indicates not a significant difference when T2 K values are compared with T3

<sup>#####</sup> Indicates a significant difference when T1 K values are compared with T3

averaging method, a larger and more evenly distributed patient population, and the usage of spasmolytic and endorectal gel is needed to verify our results.

In conclusion, our study confirmed that using a 3T scanner, the WTS-outline ROI approach could obtain the most

repeatable measurements for both non-Gaussian and Gaussian diffusion models. By using the WTS-outline method, DKI also has considerable diagnostic value for the estimation of rectal cancer characteristics, in addition to the conventional DWI model.

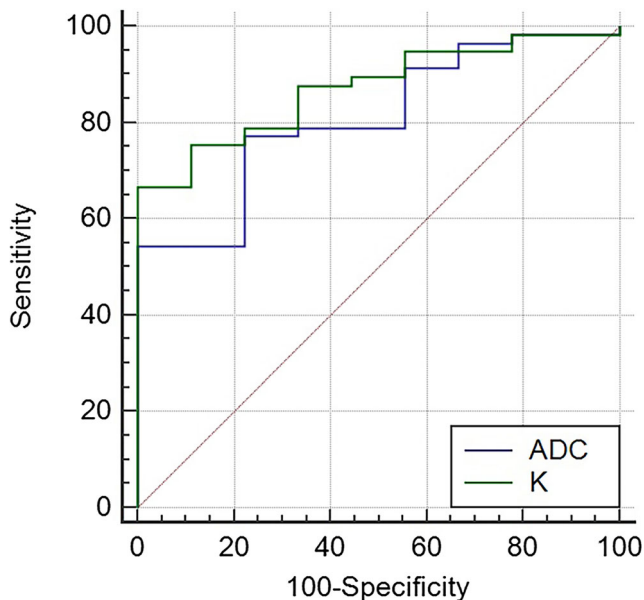


**Fig. 4** The ROC was performed to assess the well differentiated tumours using the ADC (AUC = 0.809, 95% CI: 0.693–0.895) and K values 0.871 (95% CI: 0.766–0.941). The optimal cut-off value was 0.959 for K (100% sensitivity and 66.67% specificity) and  $0.697 \times 10^{-3} \text{mm}^2/\text{s}$  for ADC (77.78% sensitivity and 77.19% specificity)

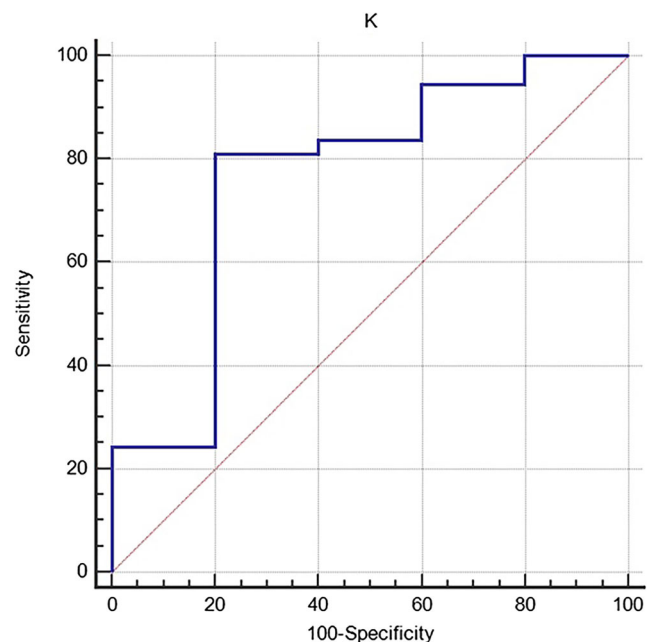


**Fig. 5** The ROC was performed to assess T2 tumours using the K values (AUC = 0.768, 95% CI: 0.592–0.914). The optimal cut-off value was 0.908 (81.1% sensitivity and 80% specificity)

**Funding** This study has received funding by the National Natural Science Foundation of China (Grant No. 81501437).

## Compliance with ethical standards

**Guarantor** The scientific guarantor of this publication is Yajia Gu.

**Conflict of interest** The authors of this manuscript declare relationships with the following companies: Siemens Shenzhen Magnetic Resonance Ltd., Shenzhen, China and MR Collaboration NE Asia, Siemens Healthineers, Shanghai, China

**Statistics and biometry** Huixun Jia, MD, Department of Clinical Statistics Center, Fudan University Shanghai Cancer Center; Department of Oncology, Shanghai Medical College, Fudan University, Shanghai, China kindly provided statistical advice for this manuscript.

**Informed consent** This was a retrospective study and did not require informed consent.

**Ethical approval** Institutional Review Board approval was obtained.

## Methodology

- retrospective
- diagnostic or prognostic study
- performed at one institution

## References

1. Van Cauter S, Veraart J, Sijbers J et al (2012) Gliomas: diffusion kurtosis MR imaging in grading. *Radiology* 263:492–501
2. Rosenkrantz AB, Sigmund EE, Johnson G et al (2012) Prostate cancer: feasibility and preliminary experience of a diffusional kurtosis model for detection and assessment of aggressiveness of peripheral zone cancer. *Radiology* 264:126–135
3. Rosenkrantz AB, Sigmund EE, Winnick A et al (2012) Assessment of hepatocellular carcinoma using apparent diffusion coefficient and diffusion kurtosis indices: preliminary experience in fresh liver explants. *Magn Reson Imaging* 30:1534–1540
4. Yu J, Xu Q, Song JC et al (2017) The value of diffusion kurtosis magnetic resonance imaging for assessing treatment response of neoadjuvant chemoradiotherapy in locally advanced rectal cancer. *Eur Radiol* 27:1848–1857
5. Hu F, Tang W, Sun Y et al (2017) The value of diffusion kurtosis imaging in assessing pathological complete response to neoadjuvant chemoradiation therapy in rectal cancer: a comparison with conventional diffusion-weighted imaging. *Oncotarget*. <https://doi.org/10.18632/oncotarget.17491>
6. Zhu L, Pan Z, Ma Q et al (2017) Diffusion Kurtosis Imaging Study of Rectal Adenocarcinoma Associated with Histopathologic Prognostic Factors: Preliminary Findings. *Radiology* 284:66–76
7. Lambregts DM, Beets GL, Maas M et al (2011) Tumour ADC measurements in rectal cancer: effect of ROI methods on ADC values and interobserver variability. *Eur Radiol* 21:2567–2574
8. Chao M, Guo X, Li L et al (2017) Effect of region of interest size on ADC measurements in pancreatic adenocarcinoma. *Cancer Imaging* 17:13
9. Colagrande S, Pasquinelli F, Mazzone LN, Belli G, Virgili G (2010) MR-diffusion weighted imaging of healthy liver parenchyma: repeatability and reproducibility of apparent diffusion coefficient measurement. *J Magn Reson Imaging* 31:912–920
10. Bickel H, Pinker K, Polanec S et al (2017) Diffusion-weighted imaging of breast lesions: Region-of-interest placement and different ADC parameters influence apparent diffusion coefficient values. *Eur Radiol* 27:1883–1892
11. Sun K, Chen X, Chai W et al (2015) Breast cancer: diffusion kurtosis mr imaging—diagnostic accuracy and correlation with clinical-pathologic factors. *Radiology* 277:46–55
12. Jensen JH, Helpert JA (2010) MRI quantification of non-Gaussian water diffusion by kurtosis analysis. *NMR Biomed* 23:698–710
13. Jensen JH, Helpert JA, Ramani A, Lu H, Kaczynski K (2005) Diffusional kurtosis imaging: The quantification of non-gaussian water diffusion by means of magnetic resonance imaging. *Magn Reson Med* 53:1432–1440
14. Edge SB, Compton CC (2010) The American Joint Committee on Cancer: the 7th edition of the AJCC cancer staging manual and the future of TNM. *Ann Surg Oncol* 17:1471–1474
15. Inoue C, Fujii S, Kaneda S et al (2014) Apparent diffusion coefficient (ADC) measurement in endometrial carcinoma: effect of region of interest methods on ADC values. *J Magn Reson Imaging JMIR* 40:157–161
16. Akashi M, Nakahusa Y, Yakabe T et al (2014) Assessment of aggressiveness of rectal cancer using 3-T MRI: correlation between the apparent diffusion coefficient as a potential imaging biomarker and histologic prognostic factors. *Acta Radiol* 55:524–531
17. Curvo-Semedo L, Lambregts DM, Maas M et al (2012) Diffusion-weighted MRI in rectal cancer: Apparent diffusion coefficient as a potential noninvasive marker of tumor aggressiveness. *J Magn Reson Imaging* 35:1365–1371
18. Sun Y, Tong T, Cai S et al (2014) Apparent Diffusion Coefficient (ADC) Value: A Potential Imaging Biomarker That Reflects the Biological Features of Rectal Cancer. *PLoS One* 9:e109371
19. Wu EX, Cheung MM (2010) MR diffusion kurtosis imaging for neural tissue characterisation. *NMR Biomed* 23:836–848